European Journal of Medicinal Chemistry 101 (2015) 552–559

Contents lists available at ScienceDirect

European Journal of Medicinal Chemistry

journal homepage: http://www.elsevier.com/locate/ejmech

Research paper

Synthesis of new 4-phenylpyrimidine-2(1*H*)-thiones and their potency to inhibit COX-1 and COX-2

Werner Seebacher [a, *], Johanna Faist [a], Armin Presser [a], Robert Weis [a], Robert Saf [b], Teresa Kaserer [c], Veronika Temml [d], Daniela Schuster [c], Sabine Ortmann [e], Nadine Otto [e], Rudolf Bauer [e]

[a] Institute of Pharmaceutical Sciences, Pharmaceutical Chemistry, University of Graz, Universitätsplatz 1, 8010 Graz, Austria
[b] Institute for Chemistry and Technology of Organic Materials (ICTM), Graz University of Technology, Stremayrgasse 9, 8010 Graz, Austria
[c] Institute of Pharmacy, Pharmaceutical Chemistry, Computer-Aided Molecular Design Group, University of Innsbruck, Innrain 80-82, 6020 Innsbruck, Austria
[d] Institute of Pharmacy, Pharmacognosy, University of Innsbruck, Innrain 80-82, 6020 Innsbruck, Austria
[e] Institute of Pharmaceutical Sciences, Pharmacognosy, University of Graz, Universitätsplatz 4, 8010 Graz, Austria

ARTICLE INFO

Article history:
Received 1 December 2014
Received in revised form
29 June 2015
Accepted 2 July 2015
Available online 10 July 2015

Keywords:
4-Phenylpyrimidine-2(1*H*)-thiones
Inhibition of cyclooxygenases

ABSTRACT

Several new 4-phenylpyrimidine-2(1*H*)-thiones have been prepared and investigated for their potencies to inhibit COX-1 and COX-2 enzymes, and COX-2 expression in THP-1 cells. Structure-activity-relationships and physicochemical parameters are discussed. Pharmacophore screening and docking studies were carried out for the most active compound.

1. Introduction

A single 4-phenylpyrimidine-2(1H)-thione has already been investigated for its analgesic, anticonvulsant and anti-inflammatory activities and was found more potent than prednisolone as anti-inflammatory agent [1]. Since the anti-inflammatory activity was described as an inhibition of plasma-PGE_2 and protection against carrageenan-induced oedema, it seemed to be interesting to investigate whether this activity is related to COX inhibition. Therefore, we prepared a series of similar compounds and determined their ability to inhibit COX-1 and COX-2 enzymes, and COX-2 expression in THP-1 cells.

2. Chemistry

The already investigated 3,4-dihydro-4-methyl-6-phenylpyrimidine-2(1*H*)-thione (**2a**) can be prepared by the reaction of 4-phenylbut-3-en-2-one (**1a**) with thiourea [2]. Alternatively, a reaction of 4-phenylbut-3-en-2-one (**1a**) with ammonium thiocyanate leads to compound **2a**, too [3]. We applied this method to prepare a series of new pyrimidinethiones **2b-2j** with various substituents at the aromatic moiety and for the synthesis of a single non-aromatic derivative **2k** to investigate the influence of the substitution patterns on the biological activity. For the preparation of compounds **2a-2j**, 4-phenylbut-3-en-2-one (**1a**) or substituted 4-arylbut-3-en-2-ones **1b-1j** were used as starting materials. The latter were prepared by aldol condensation of substituted benzaldehydes with acetone following reported procedures [4,5]. The non-aromatic pyrimidinethione **2k** was prepared from 5-methylhexen-2-one (**1k**) (Scheme 1). Evidence of structure was achieved by NMR spectroscopy. The signal of C-2 in ^{13}C NMR spectra appears at 173–175 ppm, a typical value for such thiourea

Abbreviations: BCS, biopharmaceutics classification system; CH_3OH, methanol; COX, cyclooxy-genase; DMSO, dimethylsulfoxide; EDTA, ethylenediaminetetra-acetic acid; EIA, enzyme immuno assay; ELISA, enzyme linked immunosorbent assay; GAPDH, glycerinaldehyde-3-phosphate dehydrogenase; GOLD, genetic optimization for ligand docking; LPS, lipopolysaccharide; MR, molar refractivity; MW, molecular weight; PDB, protein data base; PGE_2, prostaglandin E_2; PGHS, prostaglandin H synthase; PMA, phorbol-12-myristate-13-acetate; QED, quantitative estimate of drug-likeness; RMSD, root-mean-square deviation of atomic position; SAR, structure activity relationship; TLC, thin layer chromatography; TRIS, tris(hydroxymethyl)-aminomethane; tPSA, topological polar surface area.

* Corresponding author.
E-mail address: we.seebacher@uni-graz.at (W. Seebacher).

http://dx.doi.org/10.1016/j.ejmech.2015.07.003
0223-5234/

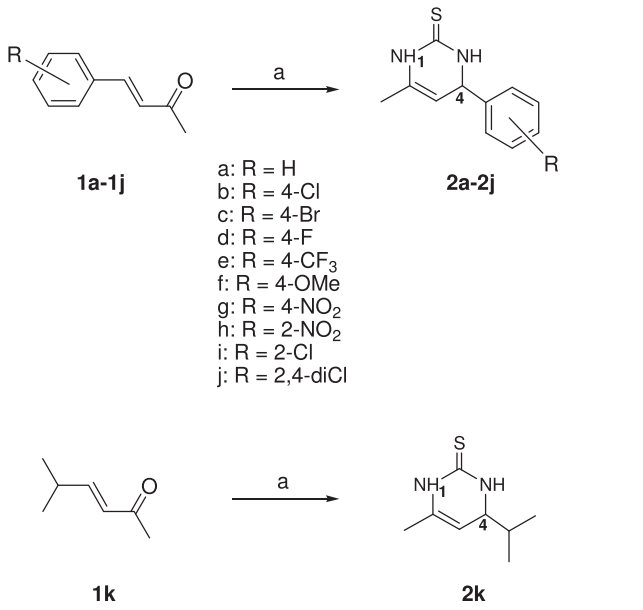

Scheme 1. Preparation of compounds **2a**–**2j**. Reagents and conditions: (a) ammonium thiocyanate, benzene, cyclohexanol, reflux 4–6 h.

structures [6]. The NH protons appear at about 8.8 and 9.7 ppm in ^{1}H NMR spectra and show long range couplings in HMBC spectra to the carbonyl carbon C-2. Furthermore, we observed w-couplings in COSY spectra of compounds **2** between both NH protons, between H-1 and H-5 and between H-5 and H-3 (Fig. 1).

3. COX-inhibition

The assays were performed in 96 well plates with purified PGHS-1 (COX-1) from rat seminal vesicles and purified PGHS-2 (COX-2) from sheep placental cotyledons (both Cayman Chemical Company, Ann Arbor, MI, USA) as previously described [7,8]. The concentration of PGE_2 was determined using a competitive PGE_2 EIA Kit (Enzo Life Sciences, Ann Arbor, MI, USA). NS-398 (Cayman Chemical Company) and indomethacin (MP Biochemicals) were used as positive controls.

For gene expression assays monocytic THP-1 cells (ECCAC, Lot No. 07I001, Sigma Aldrich) were differentiated to macrophages with 12 nM PMA for 48 h in 24-well plates, followed by incubation with test compounds, DMSO as calibrator and quercetin or dexamethasone as positive controls for NF-κB1 and COX-2 gene expression inhibition, respectively. Afterwards cells were stimulated with LPS and incubated for another three hours, except the well treated with DMSO (all Sigma Aldrich). RNA was extracted with GenElute Mammalian Total RNA Miniprep Kit (Sigma Aldrich) and reverse transcription was carried out with High Capacity cDNA Reverse Transcription Kit (Life Technologies). Relative expression was quantified via real-time PCR with TaqMan probes for NF-κB1 (NM_003998) and COX-2 (NM_000963) against endogenous control GAPDH (predesigned TaqMan assay) via ΔΔCt-method [9].

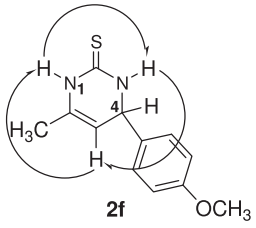

Fig. 1. W couplings in COSY spectrum of compound **2f**, marked as arrows.

4. Molecular modeling

The tested compounds were analyzed *in-silico* with two target-based methods: Pharmacophore modeling and docking. Pharmacophore models are a three-dimensional array of physicochemical features that represent the interacting functionalities of a given molecule with its target [10]. These features represent common interactions such as hydrogen bonds (H-bonds), ionic interactions, and hydrophobic interactions [11]. In principle, compounds that map a pharmacophore model, and therefore could interact in a similar manner as already known ligands, have an increased probability to be active against a specific target.

In this study, pharmacophore modeling was performed in LigandScout (version 3.02). Using this program, either a structure- or ligand-based modeling approach can be employed for the generation of pharmacophore models. In the structure-based approach, the interaction patterns of a ligand-target complex are used to calculate an initial model. In the ligand-based modeling, common pharmacophore features are extracted from three-dimensionally aligned known active molecules. These initial models can then be refined. In this study, all models were calculated based on the binding mode of co-crystallized inhibitors, because multiple ligand-target complexes were available in the Protein Data Bank [12]. If a part of the ligand fulfills the feature-specific distances, angles, and electronic requirements in relation to the protein binding site [11], a feature is placed on it. The resulting and refined 3D pharmacophore model can then be used for virtual screening. For this purpose, a 3D multi-conformational library of molecules is generated with OMEGA [13,14]. During virtual screening, LigandScout calculates a pharmacophore for each conformer and matches it to the query pharmacophore with a pattern-matching based alignment algorithm [15]. A Kabsch algorithm is used to minimize the feature distances between the query model and the conformers. Each match is evaluated with a geometrical fit value, which is calculated based on the RMSD between the fitting molecule and the pharmacophore model.

Furthermore, molecular docking was used to fit the compounds into the empty binding pocket of the target. The quality of the resulting binding poses is evaluated with a so-called docking score, which estimates the binding free energy [16]. To investigate the experimentally observed SAR, all measured compounds were screened against a previously reported pharmacophore model collection for COX-1 and COX-2 [17]. This process helped to compare the binding site interactions of the investigated compounds with the interaction patterns of well-known COX-inhibitors such as indomethacin that have been co-crystallized with the two COX isoforms. To further elucidate the binding mechanism of the novel active compound, all investigated structures were docked into the binding site of COX. The docking poses confirmed the crucial interactions from the pharmacophore model and also illustrated, why structurally closely related molecules did not display any biological activity.

5. Physicochemical properties

Physicochemical parameters are today considered to have a crucial role in the selection process of drug candidates during the early stages of drug discovery [18,19]. Most orally active drugs have a set of properties that fall in a defined physical and chemical 'drug-like space' [20–22]. For this reason an assessment of drug-likeness

for all synthesized compounds was made.

6. Results and discussion

All prepared compounds were tested for their activity to inhibit COX-1 and COX-2 enzymes. The results are presented in Table 1. Interestingly, compound **2a** does not show any inhibitory activity. The readily observed anti-inflammatory activity [1] must be the result of a different mechanism of action. Most of the compounds do not inhibit COX-1 and COX-2 with the exception of **2f**, **2g**, and **2h**. The 4-methoxy compound **2f** and the 4-nitro substituted derivative **2g** inhibit only COX-1 whereas the 2-nitro derivative **2h** shows a distinct inhibition of both cyclooxygenases. For that reason, **2h** was further investigated for its IC_{50} against COX-2 (Fig. 2) with the result, that **2h** shows a IC_{50} of around 50μM.

The parent pyrimidinethione **2a** as well as its derivative **2h** with the highest inhibitory activity were investigated for their ability to inhibit gene expression of COX-2 and NF-κB1 in THP-1 cells. The results are presented in Fig. 3. Obviously, both compounds induce gene expression of COX-2 maybe as a compensation mechanism. The expression of NF-κB1 is scarecely influenced by compounds **2a** and **2h**.

Furthermore, physicochemical properties of derivatives **2a**–**2k** were calculated to characterize them and detect possible differences which may be responsible for their differing activities. Some key physicochemical properties of compounds **2** are listed in Table 2.

All compounds comply with the drug-like classifiers defined by Lipinsky et al. [23,24], Veber et al. [25] and Ghose et al. [26]. Their molecular weight is relatively low (MW in the region of 170–283), the polar surface areas and molar refractivities are within the range where oral bioavailability and blood–brain barrier penetration is plausible [27,28].

To estimate the bioavailability of all synthesized compounds a provisional BCS classification based on *in-silico* solubility (log S) and permeability (log P) data was made [29]. Also in case of ionisable molecules the use of computed log D values, which are often difficult to determine, did not show any improvement of accuracy, therefore the general application of calculated log P for the provisional BCS classification was recommended [30].

In BCS (Biopharmaceutics Classification System) drug substances have been classified into one of four categories defined by Amidon et al. [31,32]. Most of our tested substances were found to be in BCS class I (high solubility, high permeability). The BCS is generally regarded to be one of the most significant prognostic tools created to facilitate drug discovery in recent years [33]. In addition, we calculated values that indicate the drug-likeness of the tested compounds using a published drug-likeness score (quantitative estimate of drug-likeness, QED). The QED score represents the geometric mean of eight individual functions (molecular

Table 1
Activities of **2a**–**2k**, expressed as % inhibition[a] at 50 μg/ml.

Comp.	*COX-1*	SD	*COX-2*	SD
2a	n.a	–	n.a.	–
2b	10.26	11.38	n.a.	–
2c	15.43	21.01	n.a.	–
2d	n.a	–	5.73	7.94
2e	0.92	15.72	n.a.	–
2f	33.23	15.50	10.31	9.48
2g	29.81	14.47	6.85	11.59
2h	53.00	16.93	50.99	11.95
2i	3.06	36.46	n.a.	–
2j	n.a.	–	7.33	10.72
2k	n.a.	–	n.a.	–
p.c.-1	41.47	11.05	n.t.	–
p.c.-2	n.t.	–	45.06	15.15

[a] Values represent the average of two to three determinations, n.a.: not active, n.t.: not tested. p.c.-1 positive control for COX-1 (indomethacin), p.c.-2 positive control for COX-2 (NS-398).

Table 2
Key physicochemical parameters of the synthesized compounds.

compd	MW[a]	tPSA[a] (Å^2) pH 7.4	MR[a]	Log P[a]	Log S[a]	BCS[b]	QED[c]
2a	204.29	24.06	63.91	1.96	−3.04	I	0.470
2b	238.73	24.06	68.71	2.56	−3.79	I	0.498
2c	283.19	24.06	71.53	2.73	−4.13	II	0.517
2d	222.28	24.06	64.12	2.10	−3.33	I	0.485
2e	272.29	24.06	69.88	2.84	−4.08	II	0.535
2f	234.32	33.29	70.37	1.80	−3.06	I	0.682
2g	249.29	67.2	70.23	1.90	−3.76	I	0.647
2h	249.29	67.2	70.23	1.90	−3.76	I	0.647
2i	238.73	24.06	68.71	2.56	−3.79	I	0.498
2j	273.18	24.06	73.52	3.17	−4.53	II	0.514
2k	170.27	24.06	53.04	1.48	−2.36	I	0.409

[a] The molecular weight (MW), log P, log S, topological polar surface area (tPSA) and molar refractivity (MR) were calculated using the ChemAxon software JChem for Excel 14.9.1500.912 (2014).
[b] The Biopharmaceutics Classification System (BCS) is a classification of drug substances according to their solubility and permeability properties.
[c] The quantitative estimate of drug-likeness (QED) was performed using a published drug-likeness score on a scale of 0 (not drug-like) to 1 (drug-like) based on our calculated physicochemical properties.

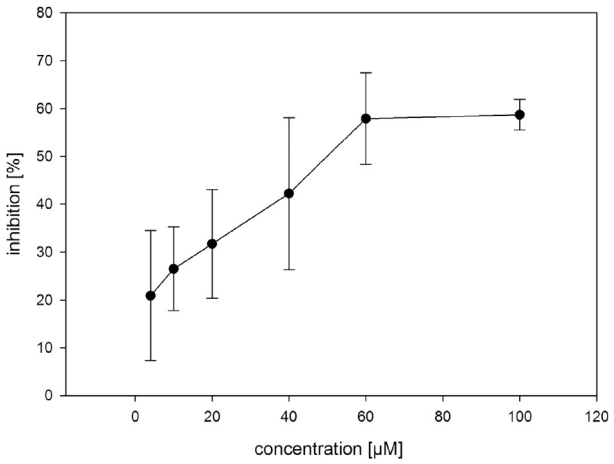

Fig. 2. COX-2: IC_{50} determination for **2h**: IC_{50}~50 μM

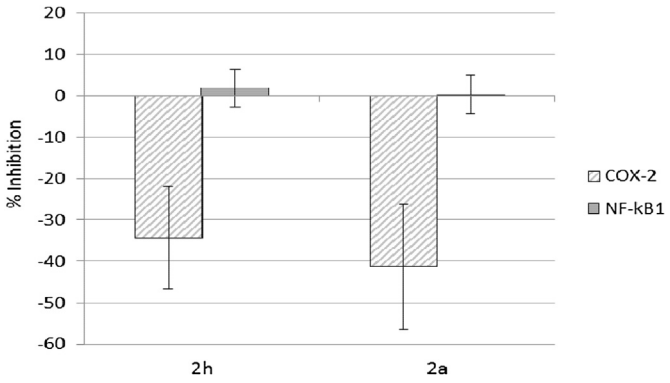

Fig. 3. Effect of **2h** and **2a** on COX-2 and NF-κB1 gene expression (concentration 50 μg/ml, n ≥ 3, mean value ± SD).

weight, octanol-water partition coefficient, number of hydrogen bond donors, number of hydrogen bond acceptors, molecular polar surface area, number of rotatable bonds, number of aromatic rings and number of structural alerts) which were selected on the basis of published precedence for their relevance in determining drug likeness [34]. QED provides an efficient means to quantify and rank the "druggability" of substances a range from 0 (not drug-like) to 1 (drug-like). In a study this common approach outperformed the Lipinsky Rule of Five, the Ghose rules and the simpler scoring system by Gleeson [35] and further performed slightly better than the Veber rule [34]. Amazingly, the computed QED score of all synthesized compounds correlates very well with the observed COX-inhibition data, particularly with regard to COX-1 ($r = 0.871$). Furthermore, there exists a significant correlation between experimental data and tPSA (COX1: $r = 0.792$ and COX-2: $r = 0.748$).

One of the pharmacophore models (based on the PDB entry 4COX [36]) found only the active constituent **2h** (Fig. 4). This model consisted of two H-bond acceptor features to Tyr355 and Arg120, respectively. In the virtual screening, these features were mapped by the nitro group in *ortho*-position, which also corresponds to the results of the docking simulation (Fig. 4). The aromatic ring and the methyl group mapped the two hydrophobic features of the model.

A detailed analysis of the interaction pattern of the docking poses revealed that all compounds formed H-bonds with Tyr385 and Ser503, respectively. Compounds **2d, 2e, 2f** and **2g** were also predicted to interact with Arg120. However, only the active compound **2h** formed an additional H-bond with Tyr355. All other compounds failed to do so, because they either had no H-bond acceptor substitution on the aromatic ring, or it was not accessible. Compound **2g**, which differs only in the substitution site of the nitro group (**2g** is para-substituted, while **2h** is *ortho*-substituted) was also inactive. Intriguingly, also **2g** was not placed in the binding site in a manner that allowed for an interaction with Tyr355 (Fig. 5).

A comparison of the binding poses of **2h** with the originally co-crystallized ligand of 4COX, indomethacin, shows that indomethacin forms additional interactions with Arg120 and Tyr355 via an ionic interaction and forms an additional H-bond with Ser530. Furthermore, it is larger and fills the hydrophobic parts of the binding pocket more thoroughly (Fig. 6).

7. Conclusion

As a surprising result, only one of the prepared compounds, 3,4-dihydro-6-methyl-4-(2-nitrophenyl)pyrimidine-2(1*H*)-thione,

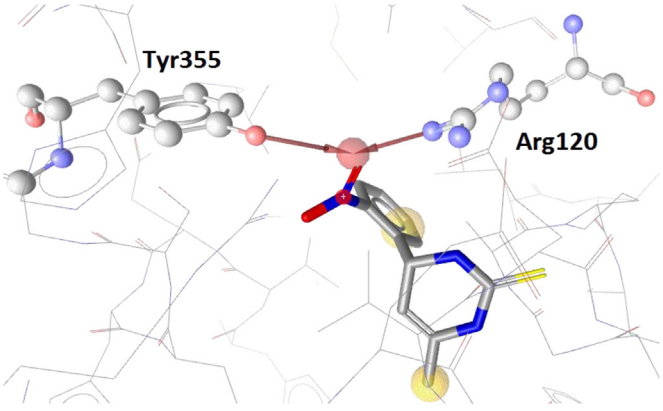

Fig. 4. Compound **2h** mapped into the pharmacophore model 4COX that found it in a virtual screening. The nitro group was predicted to form interactions with Arg120 and Tyr355. Chemical features are color-coded: H-bond – red arrow, hydrophobic contact – yellow sphere. (For interpretation of the references to colour in this figure legend, the reader is referred to the web version of this article.)

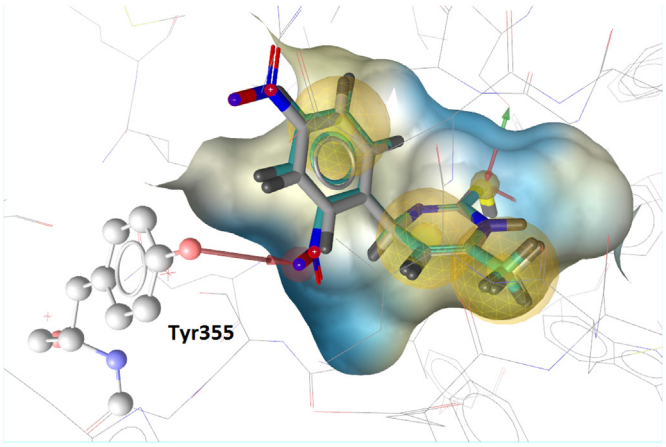

Fig. 5. Docking poses of compounds **2h** (green) and **2g** (grey). Only compound **2h** was predicted to form an H-bond with Tyr355. (For interpretation of the references to colour in this figure legend, the reader is referred to the web version of this article.)

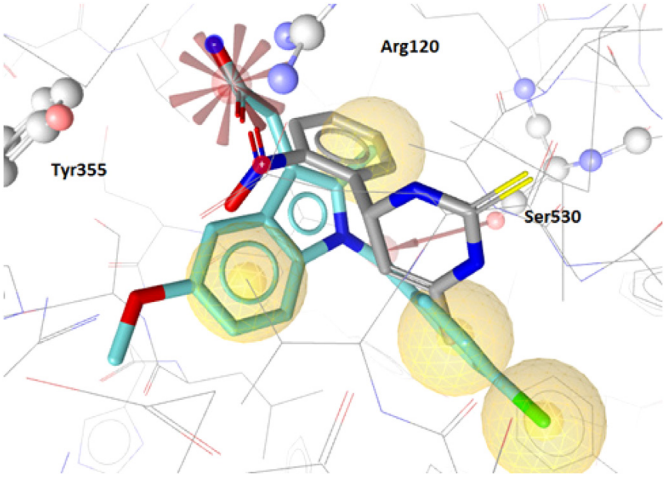

Fig. 6. Comparison between the binding of the co-crystallized inhibitor indomethacin (cyan) and **2h** (grey). Chemical interactions between indomethacin and the COX binding site are shown. The features are color-coded: H-bond – red arrow, hydrophobic contact – yellow sphere, ionic interaction – red star. (For interpretation of the references to colour in this figure legend, the reader is referred to the web version of this article.)

showed distinct inhibitory activity on cyclooxygenases. In addition, the evaluation of predictive ADMET parameters revealed the synthesized compounds to be generally drug-like and favourable for further investigations. On the other hand, it can be stated that the already observed anti-inflammatory effects of the parent compound of this investigation, 3,4-dihydro-6-methyl-4-phenylpyrimidine-2(1*H*)-thion, must be the result of a different mechanism of action than inhibition of cyclooxygenases.

8. Experimental

8.1. Instrumentation and chemicals

Melting points were obtained on a Tottoli melting point apparatus. IR spectra: infrared spectrometer system 2000 FT (Perkin Elmer). UV/VIS: Lambda 17 UV/VIS-spectrometer (Perkin Elmer) carried out in CH_3OH solutions. NMR spectra: Varian UnityInova 400 (300 K) 5 mm tubes, spectra were acquired in DMSO. Chemical shifts were recorded in parts per million (ppm), for ^1H spectra the

solvent peak (2.49) was used as internal standard and for ^{13}C spectra the central resonance line of the DMSO signal was used as the internal reference (39.7). Abbreviations: ArH, aromatic H; ArC, aromatic C; ArC_q, quaternary aromatic C, Signal multiplicities are abbreviated as follows: s, singlet; d, doublet; t, triplet; q quartet; m, multiplet. Coupling constants (*J*) are reported in Hertz (Hz). ^1H- and ^{13}C-resonances were assigned using $^1H,^1H$- and $^1H,^{13}C$-correlation spectra (gCOSY, gHSQC, gHMBC optimized on 8 Hz). ^1H- and ^{13}C-resonances are numbered as given in the formulae. HR-MS: GCT-Premier, Waters (EI, 70eV). Thin-layer chromatography (TLC): TLC plates (Merck, silica gel 60 F_{254} 0.2 mm, 200 × 200 mm); the compounds were detected in UV light at 254 nm. Solvents and reagents were obtained from commercial sources. R_f values were determined using benzene: chloroform: ethanol = 4:4:1 as eluent.

8.2. Syntheses

8.2.1. General procedure for the syntheses of 6-aryl or 6-alkyl-3,4-dihydro-4-methylpyrimidine-2(1H)-thiones (**2a-2j**)

The appropriate ketone **1** was refluxed with ammonium thiocyanate and cyclohexanol in benzene on a water separator for 4–6 h. After cooling to room temperature, the precipitate was filtered with suction, washed with ether and ethanol and dissolved in hot ethanol or hot isopropanol, treated with charcoal and filtered. Little amount of solvent was removed in vacuo and then the solution was allowed to stand overnight to complete crystallization. The products were filtered with suction washed with pure solvent and dried in vacuo over phosphorous pentaoxide. Some products were yielded in low yields, by this method. In such cases, unreacted ketone can be recovered from the filtrate of the first filtration by a concentration and crystallization process.

*8.2.1.1. (4RS)-(±)-3,4-Dihydro-6-methyl-4-phenylpyrimidine-2(1H)-thione (**2a**).* From the reaction of 12 g (*E*)-4-phenylbut-3-en-2-one **1a** (82 mmol) with 6 g ammonium thiocyanate (79 mmol) in the presence of 2.5 g cyclohexanol (25 mmol) in 35 ccm^3 of benzene, 9 g (48%) of **2a** were yielded as white crystals as described [3]. The melting point (203 °C) corresponds well with the reported one (198–199 °C) [3]. R_f = 0.50, M.p. 203 °C, IR (KBr): $\tilde{\nu}$ = 3190, 2981, 1706, 1589, 1572, 1492, 1451, 1431, 1348, 1319, 1293, 1200, 1177, 755, 696, 642 cm^{-1}; UV (CH_3OH): λ (logε) = 206 (4.252), 263 (4.058) nm; ^1H NMR ($CDCl_3$, δ, 400 MHz): 1.70 (s, 3H, CH_3), 4.72 (s, 1H, 5-H), 4.91 (s, 1H, 4-H), 7.22–7.37 (m, 5H aromatic H), 8.83 (s, 1H, 3-H), 9.57 (s, 1H, 1-H) ppm. ^{13}C NMR ($CDCl_3$, δ, 100 MHz): 17.86 (CH_3), 55.02 (C-4), 99.41 (C-5), 126.44, 127.56, 128.76 (aromatic C), 130.88 (C-6), 144.95 (aromatic C_q), 174.32 (C-2) ppm. HRMS (EI+): calcd. $C_{11}H_{12}N_2S$ [M^+]: 204.0721; found: 204.0727.

*8.2.1.2. (4RS)-(±)-4-(4-Chlorophenyl)-3,4-dihydro-6-methylpyrimidine-2(1H)-thione (**2b**).* From the reaction of 2.96 g (*E*)-4-(4-chlorophenyl)but-3-en-2-one **1b** (16.4 mmol) with 1.2 g ammonium thiocyanate (15.8 mmol) in the presence of 0.5 g cyclohexanol (5 mmol) in 50 ccm^3 of benzene, 483 mg (13%) of **2b** were yielded as white crystals. R_f = 0.56, M.p. 211 °C, IR (KBr): $\tilde{\nu}$ = 3179, 2972, 1707, 1568, 1485, 1451, 1431, 1322, 1292, 1195, 1175, 1087, 829, 783 cm^{-1}; UV (CH_3OH): λ (logε) = 204 (4.227), 263 (4.151) nm; ^1H NMR ($CDCl_3$, δ, 400 MHz): 1.70 (s, 3H, CH_3), 4.71 (s, 1H, 5-H), 4.93 (s, 1H, 4-H), 7.24 (d, *J* = 8.4 Hz, 2H, aromatic H), 7.42 (d, *J* = 8.1 Hz, 2H, aromatic H), 8.86 (s, 1H, 3-H), 9.62 (s, 1H, 1-H) ppm. ^{13}C NMR ($CDCl_3$, δ, 100 MHz): 17.86 (CH_3), 54.30 (C-4), 98.95 (C-5), 128.35, 128.75 (aromatic C), 131.27 (C-6), 132.12, 143.84 (aromatic C_q), 174.38 (C-2) ppm. HRMS (EI+): calcd. $C_{11}H_{11}ClN_2S$ [M^+]: 238.0331; found: 238.0329.

*8.2.1.3. (4RS)-(±)-4-(4-Bromophenyl)-3,4-dihydro-6-methylpyrimidine-2(1H)-thione (**2c**).* From the reaction of 1.58 g (*E*)-4-(4-bromophenyl)but-3-en-2-one **1c** (7.0 mmol) with 0.51 g ammonium thiocyanate (6.7 mmol) in the presence of 0.22 g cyclohexanol (2.1 mmol) in 25 ccm^3 of benzene, 203 mg (11%) of **2c** were yielded as white crystals. R_f = 0.47, M.p. 210 °C, IR (KBr): $\tilde{\nu}$ = 3181, 2978, 1706, 1567, 1482, 1430, 1321, 1290, 1194, 825, 782 cm^{-1}; UV (CH_3OH): λ (logε) = 205 (4.263), 264 (4.127) nm; ^1H NMR ($CDCl_3$, δ, 400 MHz): 1.70 (s, 3H, CH_3), 4.71 (s, 1H, 5-H), 4.91 (s, 1H, 4-H), 7.18 (d, *J* = 8.1 Hz, 2H, aromatic H), 7.56 (d, *J* = 8.1 Hz, 2H, aromatic H), 8.85 (s, 1H, 3-H), 9.62 (s, 1H, 1-H) ppm. ^{13}C NMR ($CDCl_3$, δ, 100 MHz): 17.85 (CH_3), 54.34 (C-4), 98.87 (C-5), 120.63 (aromatic C_q), 128.69 (aromatic C), 131.26 (C-6), 131.65 (aromatic C), 144.25 (aromatic C_q), 174.38 (C-2) ppm. HRMS (EI+): calcd. $C_{11}H_{11}BrN_2S$ [M^+]: 281.9826; found: 281.9836.

*8.2.1.4. (4RS)-(±)-4-(4-Fluorophenyl)-3,4-dihydro-6-methylpyrimidine-2(1H)-thione (**2d**).* From the reaction of 13.5 g (*E*)-4-(4-fluorophenyl)but-3-en-2-one **1d** (82 mmol) with 6.0 g ammonium thiocyanate (79 mmol) in the presence of 2.5 g cyclohexanol (25 mmol) in 35 ccm^3 of benzene, 2.7 g (15%) of **2d** were yielded as white crystals. R_f = 0.45, M.p. 199 °C, IR (KBr): $\tilde{\nu}$ = 3214, 2980, 1706, 1568, 1509, 1453, 1430, 1225, 1194, 1177, 1157, 851, 832 cm^{-1}; UV (CH_3OH): λ (logε) = 207 (4.148), 266 (4.119) nm; ^1H NMR ($CDCl_3$, δ, 400 MHz): 1.71 (s, 3H, CH_3), 4.72 (s, 1H, 5-H), 4.93 (s, 1H, 4-H), 7.16–7.28 (m, 4H, aromatic H), 8.85 (s, 1H, 3-H), 9.61 (s, 1H, 1-H) ppm. ^{13}C NMR ($CDCl_3$, δ, 100 MHz): 17.86 (CH_3), 54.26 (C-4), 99.21 (C-5), 115.51 (d, ^2J(C,F) = 21.4 Hz, aromatic C), 128.53 (d, ^3J(C,F) = 8.4 Hz, aromatic C), 131.14 (C-6), 141.18 (d, ^4J(C,F) = 2.7 Hz, aromatic C_q), 161.64 (d, ^1J(C,F) = 243.0 Hz, aromatic C_q), 174.24 (C-2) ppm. HRMS (EI+): calcd. $C_{11}H_{11}FN_2S$ [M^+]: 222.0627; found: 222.0634.

*8.2.1.5. (4RS)-(±)-3,4-Dihydro-6-methyl-4-[4-(trifluoromethyl)phenyl]pyrimidine-2(1H)-thione (**2e**).* From the reaction of 13.1 g (*E*)-4-[4-(trifluoromethyl)phenyl]but-3-en-2-one **1e** (61 mmol) with 4.5 g ammonium thiocyanate (59 mmol) in the presence of 1.9 g cyclohexanol (19 mmol) in 25 ccm^3 of benzene, 4.01 g (25%) of **2e** were yielded as white crystals. R_f = 0.46, M.p. 196 °C, IR (KBr): $\tilde{\nu}$ = 3208, 1707, 1567, 1479, 1451, 1429, 1334, 1311, 1295, 1195, 1177, 1163, 1117, 1107, 1070, 1018, 840, 785 cm^{-1}; UV (CH_3OH): λ (logε) = 207 (4.163), 264 (4.116) nm; ^1H NMR ($CDCl_3$, δ, 400 MHz): 1.70 (s, 3H, CH_3), 4.76 (s, 1H, 5-H), 5.04 (s, 1H, 4-H), 7.45 (d, *J* = 8.1 Hz, 2H, aromatic H), 7.73 (d, *J* = 8.4 Hz, 2H, aromatic H), 8.93 (s, 1H, 3-H), 9.68 (s, 1H, 1-H) ppm. ^{13}C NMR ($CDCl_3$, δ, 100 MHz): 17.85 (CH_3), 54.57 (C-4), 98.71 (C-5), 124.43 (d, ^1J(C,F) = 264.2 Hz, CF_3), 125.80 (d, ^3J(C,F) = 3.4 Hz, aromatic C), 127.17 (aromatic C), 128.17 (d, ^2J(C,F) = 31.7 Hz, aromatic C_q), 131.49 (C-6), 149.36 (aromatic C_q), 174.68 (C-2) ppm. HRMS (EI+): calcd. $C_{12}H_{11}F_3N_2S$ [M^+]: 272.0595; found: 272.0610.

*8.2.1.6. (4RS)-(±)-3,4-Dihydro-4-(4-methoxyphenyl)-6-methylpyrimidine-2(1H)-thione (**2f**).* From the reaction of 2.89 g (*E*)-4-(4-methoxyphenyl)but-3-en-2-one **1f** (16.4 mmol) with 6.0 g ammonium thiocyanate (15.8 mmol) in the presence of 0.5 g cyclohexanol (5 mmol) in 50 ccm^3 of benzene, 322 mg (9%) of **2f** were yielded as white crystals. R_f = 0.62, M.p. 184 °C, IR (KBr): $\tilde{\nu}$ = 3204, 2985, 1706, 1568, 1512, 1489, 1321, 1305, 1271, 1248, 1196, 1174, 1032, 831 cm^{-1}; UV (CH_3OH): λ (logε) = 205 (4.259), 264 (4.158) nm; ^1H NMR ($CDCl_3$, δ, 400 MHz): 1.71 (s, 3H, CH_3), 3.72 (s, 3H, OCH_3), 4.68 (s, 1H, 5-H), 4.85 (s, 1H, 4-H), 6.90 (d, *J* = 8.8 Hz, 2H, aromatic H), 7.14 (d, *J* = 8.4 Hz, 2H, aromatic H), 8.76 (s, 1H, 3-H), 9.52 (s, 1H, 1-H) ppm. ^{13}C NMR ($CDCl_3$, δ, 100 MHz): 17.88 (CH_3), 54.45 (C-4), 55.35 (OCH_3), 99.54 (C-5), 114.08, 127.84 (aromatic C), 130.79 (C-6), 137.10, 158.84 (aromatic C_q), 173.97 (C-2) ppm. HRMS

(EI+): calcd. $C_{12}H_{14}N_2OS$ [M^+]: 234.0827; found: 234.0832.

*8.2.1.7. (4RS)-(±)-3,4-Dihydro-6-methyl-4-(4-nitrophenyl)pyrimidine-2(1H)-thione (**2g**).* From the reaction of 2.73 g (*E*)-4-(4-nitrophenyl)but-3-en-2-one **1g** (14.3 mmol) with 1.05 g ammonium thiocyanate (13.7 mmol) in the presence of 0.44 g cyclohexanol (4.4 mmol) in 50 ccm^3 of benzene, 208 mg (6%) of **2g** were yielded as yellow crystals. $R_f = 0.38$, M.p. 215 °C, IR (KBr): $\tilde{\nu} = 3188$, 2980, 1712, 1607, 1572, 1522, 1490, 1429, 1351, 1320, 1289, 1200, 1175, 851, 817, 750 cm^{-1}; UV (CH_3OH): λ (logε) = 270 (4.294), 206 (4.196) nm; ^{1}H NMR ($CDCl_3$, δ, 400 MHz): 1.70 (s, 3H, CH_3), 4.77 (s, 1H, 5-H), 5.10 (s, 1H, 4-H), 7.49 (d, $J = 8.8$ Hz, 2H, aromatic H), 8.24 (d, $J = 8.4$ Hz, 2H, aromatic H), 8.98 (s, 1H, 3-H), 9.73 (s, 1H, 1-H) ppm. ^{13}C NMR ($CDCl_3$, δ, 100 MHz): 17.86 (CH_3), 54.41 (C-4), 98.29 (C-5), 124.19, 127.53 (aromatic C), 131.80 (C-6), 146.89, 152.01 (aromatic C_q), 174.78 (C-2) ppm. HRMS (EI+): calcd. $C_{11}H_{11}N_3O_2S$ [M^+]: 249.0572; found: 249.0584.

*8.2.1.8. (4RS)-(±)-3,4-Dihydro-6-methyl-4-(2-nitrophenyl)pyrimidine-2(1H)-thione (**2h**).* From the reaction of 2.96 g (*E*)-4-(2-nitrophenyl)but-3-en-2-one **1h** (16.4 mmol) with 1.2 g ammonium thiocyanate (15.8 mmol) in the presence of 0.5 g cyclohexanol (5 mmol) in 50 ccm^3 of benzene, 725 mg (20%) of **2h** were yielded as yellow crystals. $R_f = 0.47$, M.p. 207 °C, IR (KBr): $\tilde{\nu} = 3203$, 2986, 1703, 1584, 1527, 1493, 1435, 1350, 1317, 1284, 1274, 1228, 1194, 857, 784, 750, 718, 639 cm^{-1}; UV (CH_3OH): λ (logε) = 268 (3.735) nm; ^{1}H NMR ($CDCl_3$, δ, 400 MHz): 1.69 (s, 3H, CH_3), 4.83 (s, 1H, 5-H), 5.42 (s, 1H, 4-H), 7.50–7.56 (m, 2H, aromatic H), 7.84 (t, $J = 7.3$ Hz, 1H, aromatic H), 7.98 (d, $J = 8.4$ Hz, 1H, aromatic H), 8.68 (s, 1H, 3-H), 9.83 (s, 1H, 1-H) ppm. ^{13}C NMR ($CDCl_3$, δ, 100 MHz): 17.88 (CH_3), 51.29 (C-4), 97.55 (C-5), 124.66, 128.86, 129.10 (aromatic C), 132.17 (C-6), 134.76 (aromatic C), 139.69, 146.47 (aromatic C_q), 175.17 (C-2) ppm. HRMS (EI+): calcd. $C_{11}H_{11}N_3O_2S$ [M^+]: 249.0572; found: 249.0569.

*8.2.1.9. (4RS)-(±)-4-(2-Chlorophenyl)-3,4-dihydro-6-methylpyrimidin-2(1H)-thione (**2i**).* From the reaction of 14.8 g (*E*)-4-(2-chlorophenyl)but-3-en-2-one **1i** (82 mmol) with 6.0 g ammonium thiocyanate (79 mmol) in the presence of 2.5 g cyclohexanol (25 mmol) in 35 ccm^3 of benzene, 10.5 g (56%) of **2i** were yielded as white crystals. $R_f = 0.56$, M.p. 223 °C, IR (KBr): $\tilde{\nu} = 3165$, 2987, 1704, 1583, 1570, 1498, 1467, 1435, 1384, 1323, 1286, 1269, 1202, 1036, 752, 736, 641 cm^{-1}; UV (CH_3OH): λ (logε) = 207 (4.283), 264 (4.181) nm; ^{1}H NMR ($CDCl_3$, δ, 400 MHz): 1.66 (s, 3H, CH_3), 4.80 (d, $J = 1.1$ Hz, 1H, 5-H), 5.24 (s, 1H, 4-H), 7.27–7.31 (m, 2H aromatic H), 7.39–7.42 (m, 2H, aromatic H), 8.80 (s, 1H, 3-H), 9.72 (s, 1H, 1-H) ppm. ^{13}C NMR ($CDCl_3$, δ, 100 MHz): 17.83 (CH_3), 52.59 (C-4), 97.15 (C-5), 128.05, 128.13, 129.13, 129.69 (aromatic C), 129.90 (aromatic C_q), 131.62 (C-6), 141.83 (aromatic C_q), 175.35 (C-2) ppm. HRMS (EI+): calcd. $C_{11}H_{11}ClN_2S$ [M^+]: 238.0331; found: 238.0346.

*8.2.1.10. (4RS)-(±)-4-(2,4-Dichlorophenyl)-3,4-dihydro-6-methylpyrimidine-2(1H)-thione (**2j**).* From the reaction of 5.6 g (*E*)-4-(2,4-dichlorophenyl)but-3-en-2-one **1j** (26 mmol) with 1.9 g ammonium thiocyanate (25 mmol) in the presence of 0.8 g cyclohexanol (8 mmol) in 12 ccm^3 of benzene, 600 mg (9%) of **2j** were yielded as white crystals. $R_f = 0.58$, M.p. 225 °C, IR (KBr): $\tilde{\nu} = 3168$, 2986, 1704, 1580, 1560, 1490, 1468, 1434, 1385, 1322, 1202, 1105, 847 cm^{-1}; UV (CH_3OH): λ (logε) = 205 (4.511), 265 (4.124) nm; ^{1}H NMR ($CDCl_3$, δ, 400 MHz): 1.67 (s, 3H, CH_3), 4.77 (s, 1H, 5-H), 5.22 (s, 1H, 4-H), 7.26 (d, $J = 8.4$ Hz, 1H, aromatic H), 7.52 (d, $J = 8.4$ Hz, 1H, aromatic H), 7.58 (s, 1H, aromatic H), 8.82 (s, 1H, 3-H), 9.76 (s, 1H, 1-H) ppm. ^{13}C NMR ($CDCl_3$, δ, 100 MHz): 17.82 (CH_3), 52.29 (C-4), 96.68 (C-5), 128.35, 129.11, 129.48 (aromatic C), 130.89 (aromatic C_q), 131.96 (C-6), 132.76, 140.90 (aromatic C_q), 175.31 (C-2) ppm. HRMS (EI+): calcd. $C_{11}H_{10}Cl_2N_2S$ [M^+]: 271.9942; found: 271.9954.

*8.2.1.11. (4RS)-(±)-3,4-Dihydro-4-isopropyl-6-methylpyrimidin-2(1H)-thione (**2k**).* From the reaction of 9.21 g (*E*)-5-methylhex-3-en-2-one **1k** (82 mmol) with 6.0 g ammonium thiocyanate (79 mmol) in the presence of 2.5 g cyclohexanol (25 mmol) in 50 ccm^3 of benzene, 9.45 g (70%) of **2k** were yielded as white crystals. $R_f = 0.47$, M.p. 191 °C, IR (KBr): $\tilde{\nu} = 3204$, 2990, 2956, 1707, 1579, 1505, 1455, 1433, 1387, 1338, 1229, 1193, 756 cm^{-1}; UV (CH_3OH): λ (logε) = 260 (4.100), 205 (3.951) nm; ^{1}H NMR ($CDCl_3$, δ, 400 MHz): 0.76, 0.77 (2d, $J = 7.5$ Hz, 6H, $CH(CH_3)_2$), 1.56–1.66 (m, 1H, $CH(CH_3)_2$), 1.67 (s, 3H, CH_3), 3.69 (s, 1H, 4-H), 4.48 (s, 1H, 5-H), 8.29 (s, 1H, 3-H), 9.27 (s, 1H, 1-H) ppm. ^{13}C NMR ($CDCl_3$, δ, 100 MHz): 16.60, 17.03 ($CH(CH_3)_2$), 17.98 (CH_3), 34.74 ($CH(CH_3)_2$), 56.91 (C-4), 95.72 (C-5), 132.57 (C-6), 175.10 (C-2) ppm. HRMS (EI+): calcd. $C_8H_{14}N_2S$ [M^+]: 170.0878; found: 170.0892.

8.3. Determination of COX-Inhibition

The assays were performed in 96 well plates with purified PGHS-1 (COX-1) from ram seminal vesicles and purified PGHS-2 (COX-2) from sheep placental cotyledons (both Cayman Chemical Company, Ann Arbor, MI, USA). The samples were dissolved in DMSO and were tested at a concentration of 50 μg/ml. The incubation solution contained 0.1 M TRIS/HCl buffer, 18 mM epinephrinehydrogentartrate, 5 μM hematin 0.2 units/well PGHS-1 or PGHS-2 enzyme and 50 μM Na_2EDTA for the COX-2 assay. 10 μl of the samples or inhibitor/positive control were added and preincubated for 5 min at room temperature. Then 5 μM arachidonic acid dissolved in EtOH p.a. were added to start the reaction. After an incubation period of 20 min at 37 °C the reaction was stopped by adding formic acid 10%. NS-398 (Cayman Chemical Company) and Indomethacin (MP Biochemicals) were used as positive controls for the COX-2 and the COX-1 assay respectively. The concentration of PGE_2 was determined by a competitive PGE_2 EIA Kit (Enzo Life Sciences, Ann Arbor, MI, USA) which was used as described by the manufacturers. The absorbance was measured with the ELISA reader "rainbow" (TECAN). The absorbance is reversed proportional to the concentration of PGE_2. Inhibition refers to reduction of PGE_2 formation in comparison to a blank and is calculated according to the following equation:

$$inhibition\ [\%] = 100 - (conc.PGE2\ (sample) \times 100) \div (conc.PGE2\ (blank))$$

The samples were tested at least two times in duplicate in individual experiments. For the IC_{50} determination six different concentrations (4 μM–100 μM) were tested in duplicate in at least three individual experiments.

For gene expression assay, THP-1 cells were cultivated in 24-well plates in media supplemented with PMA at a final concentration of 12 nM in order to differentiate the monocytes to macrophages. After 48 h cells were treated with compounds (50 μg/ml) and incubated for one hour. One well was treated with 0.1% dimethylsulfoxide (DMSO) (Sigma Aldrich®) for calibration. Quercetin (25 μM) and/or dexamethasone (2.5 nM) were applied as positive controls. After one hour cells were stimulated with Lipopolysaccharide (LPS) (O55:B5, 7.5 ng/ml, Sigma Aldrich®) - except the well treated with DMSO − and incubated for another three hours. *RNA isolation*: medium was removed and adherent cells were washed twice with cold PBS in order to remove remaining monocytes. Extraction of RNA was carried out with Gen Elute™ Mammalian Total RNA Miniprep Kit (Sigma Aldrich®). Lysis solution/2-mercaptoethanol (mixture prepared according to manufacturer's instructions) was applied directly onto adherent cells. Lysate was mixed by pipetting and transferred into a GenElute™ filtration column. Wells were rinsed with 100 μl lysis solution and the

solution was added to the filtration column. Subsequent extraction steps were performed according to manufacturer's protocol. The purified total RNA was used instantly for reverse transcription and was afterwards stored at −80 °C. *Reverse transcription*: total RNA was reversely transcribed into cDNA by means of High Capacity cDNA Reverse Transcription Kit™ (Life Technologies, Carlsbad, CA, USA) on a Mastercycler personal (Eppendorf, Hamburg, Germany). *Real-time PCR*: quantification of the synthesized cDNA was performed with reagents from Life Technologies: TaqMan™ Universal PCR Master Mix (no AmpErase® UNG), pre-developed TaqMan™ assay for human Glyceraldehyde 3-phosphate dehydrogenase (GAPDH), TaqMan™ probes with FAM™ label as well as sequence detection primers. Each sample was applied and measured in duplicate in 96-well PCR plates. PCR and fluorescence detection were performed with 7300 ABI real-time PCR system (Applied Biosystems, nowadays incorporated into Life Technologies). Gene expression was relatively quantified against the endogenous control gene GAPDH via ΔΔCt-method and analysed with SDS software version 1.2.1.

8.4. Molecular modeling

All calculations were performed on a multi-core workstation with 2.4 + GHz, 8 GB of RAM, and a high-end NVIDIA graphical processing unit.

8.4.1. Pharmacophore modeling

All compounds and their tautomeric states were screened in LigandScout 3.03b [11] against a set of previously developed pharmacophore models described in Temml et al. [17]. 500 conformations were calculated for each tautomer of the structures with OMEGA version 2.3.3 [13,14], implemented in LigandScout.

8.4.2. Docking studies

The crystal structure of methyl flurbiprofen in complex with COX-1 (PDB entry 1HT5, [37]) was employed for the docking studies with GOLD version 5.1 [38]. For validation of the docking parameters, the co-crystallized ligand was again docked into the binding site, and the predicted pose retrieved a RMSD value of 1.03 Å. Subsequently, the whole database of compounds (including tautomeric states) was docked. The interaction patterns of the highest ranked docking pose of every compound were manually analyzed in LigandScout 3.03b.

Acknowledgements

We thank the Austrian Science Fund (FWF) National Research Network (NFN) Project “Drugs from nature targeting inflammation” (S10711), the foundation “Verein zur Förderung der wissenschaftlichen Ausbildung und Tätigkeit von Südtirolern an der Landesuniversität Innsbruck”, and the Erika Cremer Habilitation Program of the University of Innsbruck for financial support. We also thank OpenEye and Inte:Ligand for providing software free of charge.

Appendix A. Supplementary data

Supplementary data related to this article can be found at http://dx.doi.org/10.1016/j.ejmech.2015.07.003.

References

[1] S.A. Said, A. El-G, E. Amr, N.M. Sabry, M.M. Abdalla, Analgesic, anticonvulsant and ant-inflammatory activities of some synthesized benzodiazepine, triazolopyrimidine and bis-imide derivatives, Eur. J. Med. Chem. 44 (2009) 4787–4792.
[2] A.-M.A. Sammour, M.M. El-Deen, A.-el-H.M. Nonr, Condensation of unsaturated ketones with thioureas, U.A.R. J. Chem. 13 (1970) 7–24.
[3] G. Zigeuner, H. Brunetti, H. Ziegler, M. Bayer, Dihydro-6-methyl-(or -6-styryl-)-4-phenyl-2(*1H*)-pyrimidinones (-thiones); Hexahydro-5-benzoyl- (or -cinnamoyl-)-4,7-diphenyl-2(*1H*)-quinazolinones (-thiones), Chem. Mon. 101 (1970) 1767–1787.
[4] Y. Tamura, Nonsteroidal antiinflammatory agents. 1. 5-Alkoxy-3-biphenylylacetic acids and related compounds as new potential antiinflammatory agents, J. Med. Chem. 20 (1977) 709–714.
[5] T. Nishimura, Antituberculous compounds. II. Thiosemicarbazones from Benzalacetones, Bull. Chem. Soc. Jpn. 26 (1953) 253–254.
[6] H.O. Kalinowski, S. Berger, S. Braun, ^{13}C-NMR-Spektroskopie, Georg Thieme Verlag, Stuttgart, New York, 1984.
[7] B.L. Fiebich, M. Grozdeva, S. Hess, M. Hüll, U. Danesch, A. Bodensieck, R. Bauer, *Petasites hybridus* extracts in vitro inhibit COX-2 and PGE2 release by direct interaction with the enzyme and by preventing microglial cells, Planta Med. 71 (2005) 12–19.
[8] E.A. Reiniger, R. Bauer, Prostaglandin-H-synthase (PGHS)-1 and -2 microtiter assays for testing of herbal drugs and in vitro inhibition of PGHS-isoenzyms by polyunsaturated fatty acids from *Platycodi radix*, Phytomedicine 13 (2006) 164–169.
[9] K.J. Livak, T.D. Schmittgen, Analysis of relative gene expression data using real-time quantitative PCR and the 2-ΔΔCT Method, Methods 25 (2001) 402–408.
[10] C.G. Wermuth, C.R. Ganellin, P. Lindberg, L.A. Mitscher, Glossary of terms used in medicinal chemistry (IUPAC recommendations 1998), Pure Appl. Chem. 70 (1998) 1129–1143.
[11] G. Wolber, T. Langer, LigandScout: 3-D pharmacophores derived from protein-bound ligands and their use as virtual screening filters, J. Chem. Inf. Model 45 (2005) 160–169.
[12] H. Berman, J. Westbrook, Z. Feng, G. Gilliland, T. Bhat, H. Weissig, I. Shindyalov, P. Bourne, The protein data bank, Nucleic Acids Res. 28 (2000) 235–242.
[13] P.C.D. Hawkins, A.G. Skillman, G.L. Warren, B.A. Ellingson, M.T. Stahl, Conformer generation with OMEGA: algorithm and validation using high quality structures from the Protein Databank and Cambridge Structural Database, J. Chem. Inf. Model 50 (2010) 572–584.
[14] P.C.D. Hawkins, A. Nicholls, Conformer generation with OMEGA: learning from the data set and the analysis of failures, J. Chem. Inf. Model 52 (2012) 2919–2936.
[15] G. Wolber, A.A. Dornhofer, T. Langer, Efficient overlay of small organic molecules using 3D pharmacophores, J. Comput. Aided Mol. Des. 20 (2006) 773–788.
[16] D.B. Kitchen, H. Decornez, J.R. Furr, J. Bajorath, Docking and scoring in virtual screening for drug discovery: methods and applications, Nat. Rev. Drug Discov. 3 (2004) 935–949.
[17] V. Temml, T. Kaserer, Z. Kutil, P. Landa, T. Vanek, D. Schuster, Pharmacophore Modeling for Cyclooxygenase-1 and 2 inhibitors with LigandScout in comparison to Discovery Studio, Fut. Med. Chem. 6 (2014) 1869–1881.
[18] H. van de Waterbeemd, E. Gifford, ADMET in silico modeling: towards prediction paradise? Nat. Rev. Drug Discov. 2 (3) (2003) 192–204.
[19] M.S. Lajiness, M. Vieth, J. Erickson, Molecular properties that influence oral drug-like behavior, Curr. Opin. Drug Discov. Dev. 7 (4) (2004) 470–477.
[20] M.C. Wenlock, R.P. Austin, P. Barton, A.M. Davis, P.D. Leeson, A comparison of Physiochemical Property Profiles of development and Marketed oral drugs, J. Med. Chem. 46 (7) (2003) 1250–1256.
[21] J.D. Hughes, J. Blagg, D.A. Price, S. Bailey, G.A. DeCrescenzo, R.V. Devraj, E. Ellsworth, Y.M. Fobian, M.E. Gibbs, R.W. Gilles, N. Greene, E. Huang, T. Krieger-Burke, J. Loesel, T. Wager, L. Whiteley, Y. Zhang, Physiochemical drug properties associated with in vivo toxicological outcomes, Bioorg. Med. Chem. Lett. 18 (17) (2008) 4872–4875.
[22] C.A. Lipinski, A. Hopkins, Navigating chemical space for biology and medicine, Nat. (London, U. K.) 432 (7019) (2004) 855–861.
[23] C.A. Lipinski, F. Lombardo, B.W. Dominy, P.J. Feeney, Experimental and computational approaches to estimate solubility and permeability in drug discovery and development settings, Adv. Drug Deliv. Rev. 23 (1–3) (1997) 3–25.
[24] C.A. Lipinski, Lead- and drug-like compounds: the rule-of-five revolution, Drug Discov. Today: Technol. 1 (4) (2004) 337–341.
[25] D.F. Veber, S.R. Johnson, H.-Y. Cheng, B.R. Smith, K.W. Ward, K.D. Kopple, Molecular properties that influence the oral bioavailability of drug candidates, J. Med. Chem. 45 (12) (2002) 2615–2623.
[26] A.K. Ghose, V.N. Viswanadhan, J.J. Wendoloski, A knowledge-based approach in designing combinatorial or medicinal chemistry libraries for drug discovery. 1. A qualitative and quantitative characterization of known drug databases, J. Comb. Chem. 1 (1) (1999) 55–68.
[27] H. Pajouhesh, G.R. Lenz, Medicinal chemical properties of successful central nervous system drugs, NeuroRx 2 (4) (2005) 541–553.
[28] H. van de Waterbeemd, Physicochemical approaches to drug absorption, in: R. Mannhold, H. Kubinyi, G. Folkers, H. van de Waterbeemd, B. Testa (Eds.), Drug Bioavailability, Wiley-VCH Verlag GmbH & Co. KGaA, Weinheim, Germany, 2008, pp. 69–99.
[29] K.J. Box, J. Comer, Using measured pKa, LogP and solubility to investigate supersaturation and predict BCS class, Curr. Drug Metab. 9 (9) (2008)

869–878.
[30] A. Dahan, O. Wolk, Y.H. Kim, C. Ramachandran, G.M. Crippen, T. Takagi, M. Bermejo, G.L. Amidon, Purely in silico BCS classification: science based quality standards for the world's drugs, Mol. Pharm. 10 (11) (2013) 4378–4390.
[31] G.L. Amidon, H. Lennernaes, V.P. Shah, J.R. Crison, A theoretical basis for a biopharmaceutic drug classification: the correlation of in vitro drug product dissolution and in vivo bioavailability, Pharm. Res. 12 (3) (1995) 413–420.
[32] A. Dahan, J.M. Miller, G.L. Amidon, Prediction of solubility and permeability class membership: provisional BCS classification of the world's top oral drugs, AAPS J. 11 (4) (2009) 740–746.
[33] G.L. Amidon, H. Lennernas, V.P. Shah, J.R. Crison, A theoretical basis for a biopharmaceutic drug classification: the correlation of in vitro drug product dissolution and in vivo bioavailability, Pharm Res 12, 413-420, 1995-Backstory of BCS, AAPS J. 16 (5) (2014) 894–898.
[34] G.R. Bickerton, G.V. Paolini, J. Besnard, S. Muresan, A.L. Hopkins, Quantifying the chemical beauty of drugs, Nat. Chem. 4 (2) (2012) 90–98.
[35] M.P. Gleeson, A. Hersey, D. Montanari, J. Overington, Probing the links between in vitro potency, ADMET and physicochemical parameters, Nat. Rev. Drug Discov. 10 (3) (2011) 197–208.
[36] R.G. Kurumbail, A.M. Stevens, J.K. Gierse, J.J. McDonald, R.A. Stegeman, J.Y. Pak, D. Gildehaus, J.M. Miyashiro, T.D. Penning, K. Seibert, Structural basis for selective inhibition of cyclooxygenase-2 by anti-inflammatory agents, Nature 384 (1996), 664–648.
[37] B.S. Selinsky, K. Gupta, C.T. Sharkey, P.J. Loll, Structural analysis of NSAID binding by protaglandine H2 synthase: time-dependent and time-independent inhibitors elicit identical enzyme conformations, Biochemistry 40 (2001) 5172–5180.
[38] G. Jones, P. Willett, R.C. Glen, A.R. Leach, R. Taylor, Development and validation of a genetic algorithm for flexible docking, J. Mol. Biol. 267 (1997) 727–748.